Solid Freeform Fabrication 2016: Proceedings of the 27th Annual International Solid Freeform Fabrication Symposium – An Additive Manufacturing Conference
Reviewed Paper

SELECTIVE LASER SINTERING OF LOW DENSITY, LOW COEFFICIENT OF THERMAL EXPANSION SILICA PARTS

John M. Hostetler[i], Jonathan T. Goldstein[ii], Augustine M. Urbas[ii], Rodrigo E. Gutierrez[iii], Theresa E. Bender[i], Charles S. Wojnar[i], Edward C. Kinzel[i]

[i]Department of Mechanical and Aerospace Engineering, Missouri University of Science and Technology, Rolla, MO
[ii]Air Force Research Laboratory, Materials and Manufacturing Directorate, Wright-Patterson Air-Force Base, OH
[iii]AmericaMakes, Youngstown OH, and Department of Mechanical Engineering, Youngstown State University, Youngstown, OH

Abstract

This paper presents a study of selective laser sintering of silica-gel. The objective of this work is to investigate a technique to create free-form, low to zero coefficient of thermal expansion structures. This offers potential cost savings over the conventional casting of large pieces of glass-ceramic followed by machining lightening features. In this paper, A CO_2 laser is coupled through a gantry system and focused onto a binder-free silica-gel powder bed (15-40 μm particles). Prior to writing each layer, powder is dispensed by sifting it onto the build platform as opposed to a conventional wiper system. This avoids contacting and potentially damaging sensitive parts. After deposition, the parts are annealed in a furnace to increase their strength. The influence of various process parameters including scan speed and laser power on final shape is investigated. In addition, the flexural strength of annealed parts is measured via three-point bending tests.

Introduction

Selective Laser Sintering (SLS) is a powder-based additive manufacturing process which utilizes a laser to locally heat powdered material, thus fusing particles in accordance with a two-dimensional pattern created within a modeling program. The deposition of consecutive powder layers then allows for the fabrication of complex three-dimensional parts, which are in turn supported by previously sintered layers and the surrounding powder itself[1]. While the SLS of metals and polymers has been investigated and documented extensively[2-3], the adaption of SLS platforms for the fabrication of ceramic structures has received very little attention, due in part to complications resulting from the process's fast cooling cycles[1]. Additionally the SLS of brittle materials often results in the formation of cracks in the part during the building process, and any ceramic parts which are successfully fabricated exhibit mechanical strengths much lower than those of conventional ceramics[4].

The SLS process traditionally operates through the atomic diffusion and binding of the structural powder at temperatures well below its melting point[5]. However, a solid binder may be utilized to aid in the manufacturing of ceramic parts, where the binder is mixed with the ceramic powder and is subsequently melted by the laser, thus enveloping the ceramic powder via capillary forces. However, this method does not melt the ceramic powder itself, and therefore requires an additional step wherein the fabricated part is heated in a furnace to impart strength to

the structure; or depending on the application, remove the binder from the part all together[1]. However, another category of SLS has potential for fabricating 3D geometries without using a binding material. Solid State Sintering (SSS) is a thermal process which occurs at temperatures ranging from $T_{melt}/2$ and T_{melt}, where T_{melt} is the melting temperature of the material. Therefore SSS encourages atomic diffusion within the powder, meaning that this process is applicable for a wide range of materials provided the platform is capable of reaching the required temperature [6].

Additionally, conventional SLS platforms rely on rollers or wipers to deposit additional powder layers, allowing for the rapid manufacturing of functional parts. However these distribution techniques are negatively impacted by the particle geometry of the powder being spread, and the roller/wiper often damages the fragile structure sintered in the previous powder layer. In addition, the quality of parts fabricated with SLS increases when the grain size of the powdered material decreases. However, the frequency of agglomerations on the sintered surface increases with a decreasing grain size, making further powder layer depositions impossible with a conventional wiper or blade[7]. Attention has been given to improving the conventional powder spreading process by studying the impact of the wiper/roller motions on the density and homogeneity of the resulting powder layer, but at present the most effective means of achieving a more homogeneous powder layer is to compress the powder as it is being spread[8], which only serves to further increase the direct shear loading on the sintered structure below.

This study aims to fabricate functional silica gel parts via SLS/SSS (with no binding agent), and in doing so investigate alternative powder distribution techniques which operate in a manner to enable the rapid manufacturing of three-dimensional parts, and which also offer advantages over the conventional wiper/roller approach. Once parts are successfully fabricated, they will then be characterized to identify the SLS platform parameters that result in the highest dimensional accuracy and structural integrity of the fabricated parts. Moreover, annealing parts after deposition is investigated as a means for increasing mechanical strength.

Material Fabrication

The SLS platform used in these experiments is based on a repurposed laser cutting system equipped with a 40 W CO_2 laser (see Fig. 1.a). A three mirror assembly directs the laser, with the last mirror fixed to a carriage that is positioned on a translational rail that deflects the beam downwards by ninety degrees, through a lens onto the powder bed (Fig. 1.b). The SLS process takes place in a room temperature laboratory environment and the laser has a spot measured size of 254 μm at the substrate. The parameters varied to effect the quality of the sintered structure were the laser power [W] and scan speed [mm/s].

Fig. 1.a. Experimental SLS platform

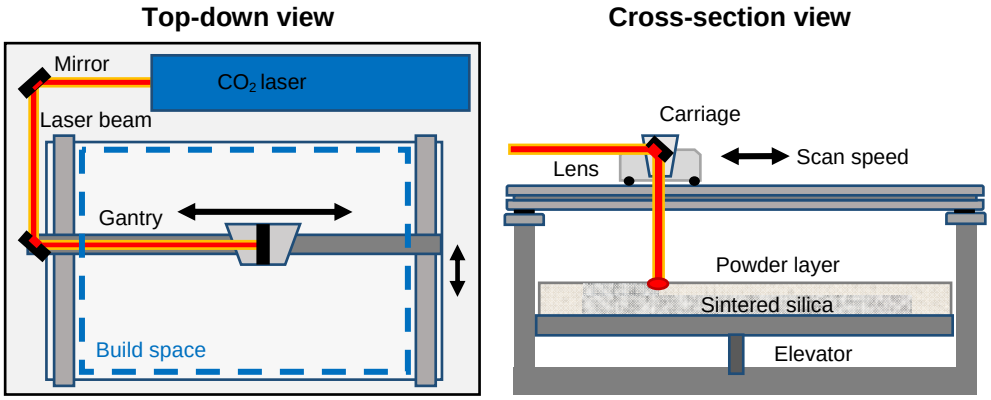

Fig. 1.b. Powder bed AM technique diagram

Small granular particles are preferred for the powder as these powders require less energy to melt and improve the surface quality of the sintered surface[9]. Therefore, silica gel (Silica P-Prep TLC Premium RF) was selected with these considerations in mind and also for its low coefficient of thermal expansion (CTE) of approximately 10^{-6}/°C. The silica gel has a particle size of 15-40 µm, a bulk density of 0.5 g/cm^3, and a porosity of 60 Å. The silica powder was then deposited onto a 75×25 mm quartz slide which acted as a substrate.

Powder distribution technique

The silica powder was distributed via a sifter technique, which utilizes a silica-filled container with a fine mesh on the bottom. The vessel is then vibrated, which results in the powder being sifted out onto the substrate below; resulting powder layers are distributed with a thickness of 0.65 ± 0.15 mm. While conventional SLS platforms deposit powder layers by spreading the powder across the build area with a wiper; and frequently damaging the fragile sintered structure below, the sifter distribution technique benefits from the ability to quickly deposit additional layers of powder without subjecting the sintered structure to shear loading during the deposition process. Additionally, while the conventional method of spreading powder with a wiper is sensitive to the geometry of the silica particles [1], the shaker technique was found to be equally capable of distributing granular particles as it is spherical particles.

Perhaps the most critical powder bed characteristic associated with strong, cohesive structures is the consistency in thickness of the distributed powder layers. By decreasing the

powder layer thickness as much as possible, consecutive sintered layers are more likely to solidify as a single structure. If the powder layer thickness varies from one deposition to the next, so too will the cohesive strength of the sintered layers. In some cases, if a single powder layer is too thick, structural unification is lost and the final part separates along that particular layer. Additionally, a reduction in the powder layer thickness allows for a higher scan speed, as the depth of sintering required to fuse particles to the previous layer is reduced[9]. However, too thin of a powder layer risks a stepping effect[10], wherein the sintering depth exceeds the powder layer and decreases dimensional accuracy. Therefore a decreasing powder layer depth must correspond to a decrease in laser power or an increase in scan speed. A study by Bertrand et al. stipulates that the powder layer thickness should be ten times greater the average particle diameters[8].

Results and Discussion

Dimensional accuracy

To precisely design the shape of SLS parts, it is important to determine the appropriate laser power and scanning speed. In particular, these parameters change the sintered area of the powder due to different temperature distributions. This affects the final geometry of the part and can lead to deviations from the desired shape. The effect of different combinations of laser power and scan speed on the accuracy of the resulting specimen geometry was investigated. Single layer square patterns with a 0.75 mm height and different specified widths, w_0, of 5, 10, and 15 mm were deposited using the system. The width of the deposited structures, w, was measured for different combinations of laser power and scan speed. The results showed that for the same ratio of laser power to scan speed, a consistent amount of powder is fused along the boundary of the desired sintered region, regardless of the size of the pattern, which was also observed in previous studies[11]. Therefore, the width of the sintered region can be modeled using the expression $w=w_0+\delta$, were δ is the error in the width dimension and is a function of laser power and scan speed.

The error in the dimensions of 10×10 mm^2 square patterns with a 0.75 mm height was determined for several combinations of laser power and scan speed. The scan speed was varied from 100 mm/s to 300 mm/s in 50 mm/s increments while maintaining one of several iterations of specified laser power. The dimensions of the sintered regions were measured with electronic calipers, and the values of δ were determined for different ratios of laser power to scan speed (Fig. 2).

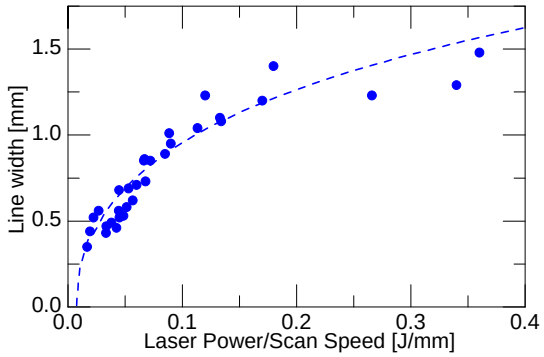

Fig. 2. Dimensional excess associated with different ratios of laser power to scan speed

The trend of the line width versus the ratio of laser power to scan speed shown in Fig. 2 supports the theory that the dimensional excess of sintered parts is a result of energy flux from the laser spot to surrounding particles. This energy flux causes particles adjacent to the laser spot to melt. Increasing the power supplied to the laser increases the energy flux density and a larger area of particles surrounding the laser beam is melted. This conclusion is corroborated by Klocke et al., who found that increasing the laser power leads to an increase in the density of the specimen, as well as creating a larger melt pool[9].

Densification

A phenomena observed to be present in every test of the SLS platform is that when a region of powder is sintered, there is a subsequent height difference between the sintered surface and the surrounding powder bed as shown in Fig. 3. These regions are consistently recessed within the powder bed by 0.12 ± 0.06 mm when sintered with a laser power of 19.5 W and a 200 mm/s scan speed.

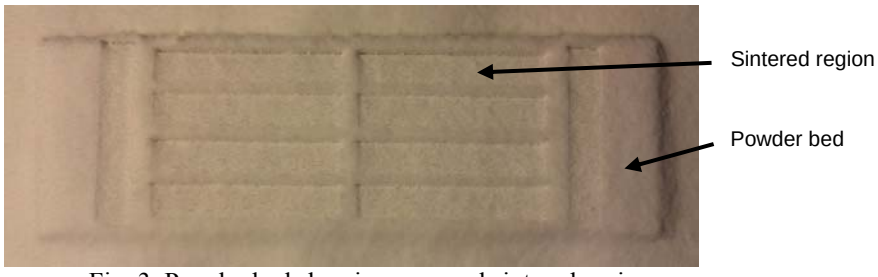

Fig. 3. Powder bed showing recessed sintered regions

The depressed nature of the sintered pattern complicates the construction of three-dimensional shapes that include variations in its cross-sectional area along the height of the structure; if a sintered pattern includes an area of previously un-sintered powder bed, the desired outcropping will be formed at a greater height than previously sintered regions connected to it. This results in a wavy surface.

The density of the sintered silica is 0.41 g/cm^3 on average. This constitutes a decrease in density of approximately 18% from the theoretical density. If the height difference between sintered regions and the surrounding powder bed was the result of densification occurring during the sintering process, Eq. (1) would predict the height ratio of the sintered region to the powder bed by assuming that the mass, length, and width of the region remain constant. Eq. (1) dictates however that if the height of the sintered region decreases, then it is required that the density of the sintered silica increases. By weighing the powder bed before and after a region is sintered, it has been determined that there is a mass loss of 0.0146 ± 0.0032 g when sintering using a laser power of 19.5 W and a scan speed of 200 mm/s. By taking this mass loss into account, it is possible that the recessed height of sintered regions is the result of densification occurring during the sintering process. Explaining this loss of mass is still subject to ongoing research.

$$\frac{h_{sinter}}{h_{powder}} = \frac{\rho_{powder}}{\rho_{sinter}} \tag{1}$$

It has also been observed that when the laser begins to sinter a region of unfused powder, there is a significant amount of densification occurring along the pattern where the laser first traverses (see Fig. 4). These depressed regions are almost entirely confined to a thin layer of the fused pattern in the negative-y direction, as these are the regions in which the laser first begins to sinter the powder bed.

Fig. 4. Densification band in the powder bed

The laser power was decreased to determine if thickness of the densified bands could be reduced. In the interest of preserving the mechanical strength of the sintered silica, the laser power-to-scan speed ratio corresponding to a qualitatively optimal sintered silica part (19.5/200 [J/mm]) was preserved as the power was decreased. The thickness of the densification band present for each of the laser powers tested were then measured and are shown in Fig. 5.

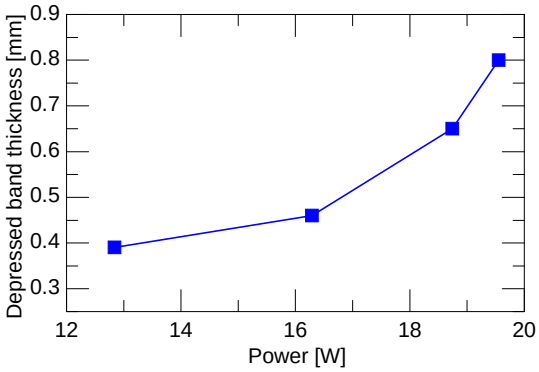

Fig. 5. Effect of laser power on densification band thickness

Due to the porosity of parts fabricated using SLS, their mechanical strength is reduced. In order to increase strength by increasing density, SLS parts were annealed at various temperatures. Several sintered silica bar samples were weighed and their dimensions recorded before they were annealed in an oven at a specified temperature for a soak time of thirty minutes. After being slowly cooled down to room temperature at a rate of 1°C per minute to avoid incurring destructive thermal stresses, the dimensions of the bars were again measured and the parts weighed. SEM images taken of silica samples post-fabrication and post-annealing reveal that the annealing process does little to decrease the porosity of the parts (Fig. 7). The estimated densification resulting from annealing the silica samples at temperatures ranging from 1000-1400°C is depicted in Fig. 8. A maximum density of 0.66 g/cm^3 results from annealing the silica at 1250°C, after which the density plateaus for higher annealing temperatures.

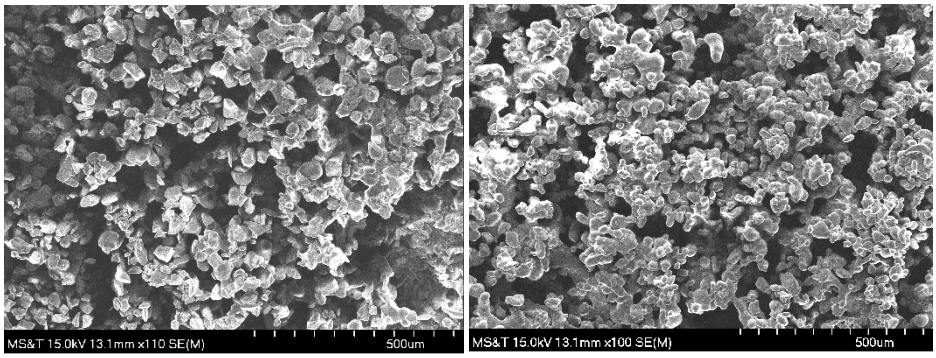

Fig. 7. SEM images of sintered silica post-deposition (left) and post-annealing at 1400 °C (right)

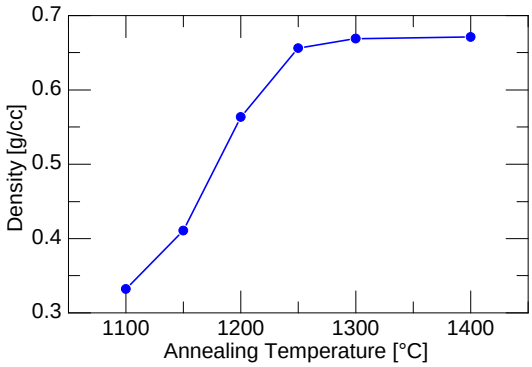

Fig. 8. Densification resulting from annealing silica samples

Flexural Strength Testing

The flexural strength of sintered and annealed silica beams with rectangular cross-sections of 4×3×20 mm^3, were measured in accordance with ASTM standards[12]. In determining the flexural strength of the ceramic specimens produced via SLS, a three-point bending test was utilized with a fully-articulating fixture. The flexural strength of the specimens were determined via Eq. (2)[12]

$$S = \frac{3PL}{2bd^2} \tag{2}$$

where P is the maximum load present at failure, L is the unsupported span of the test specimen, b is the specimen width, and d is the specimen thickness. Failure was identified by a 50% decrease in applied load corresponding to a near-constant value of deflection. Note that the dimensions used in Eq. (2) are those measured post-annealing, and not the nominal dimensions.

The flexural strength of silica samples annealed over a range of temperatures is plotted in Fig. 9. An annealing temperature of 1250°C results in a maximum mean flexural strength of 3.165 MPa for a sample size of ten beams. However the flexural strength then decreased to approximately 50% of this maximum value when annealing at temperatures greater than 1250°C. Whether or not this drop in strength is due to a crystallization which takes place which is subsequently degraded at higher temperatures, or some other effect of the material behavior, is

unknown at this time. However it is possible that the soak time of thirty minutes when annealing is not sufficient for imparting a maximum amount of strength to the samples, which may also explain why the densification of the silica plateaus around this same anneal temperature of 1250°C.

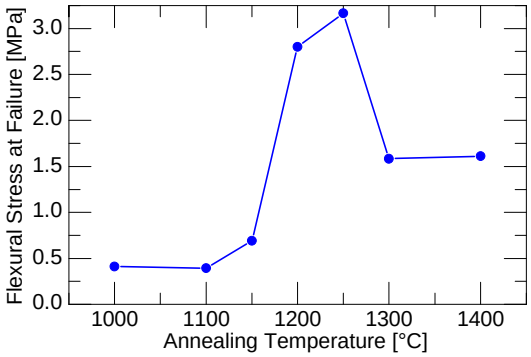

Fig. 9. Flexural strength of silica samples annealed at various temperatures

Fig. 10. Fractured silica beams post three-point bending test

The fracture surfaces of specimens after failure (shown in Fig. 10) exhibit jagged cracks. The cracks propagated from one powder layer to the next; resulting in localized peaks in the load vs. deflection plot that correspond to individual powder layer fractures (see Fig. 11). The crack propagation through a fracturing specimen may be altered to more closely resemble traditional behaviors of conventional linear elastic, homogeneous materials by decreasing the powder layer thickness, which improves the likelihood of a cohesive bond with the substrate below. However, decreasing the powder layer thickness necessitates that more layers be deposited overall to produce a part with the same height, which decreases the productivity of the platform

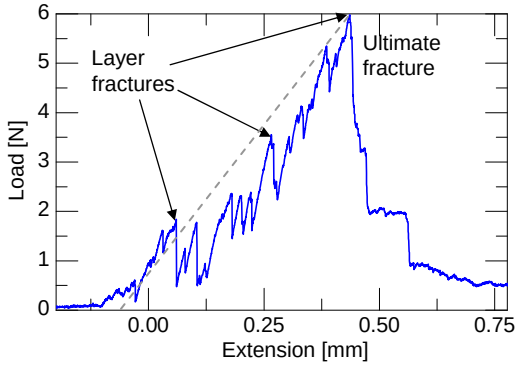

Fig. 11. Characteristic load vs. deflection experimental data for fractured silica samples

An alternative approach used in previous studies[6] for increasing the strength of SLS parts is to decrease the laser scan speed of the platform, which increases the duration of the heat flux. However, this trend was not observed in the present study. Silica beams fabricated with scan speeds identified to be ± 25% of an ideal speed were annealed and tested to determine their

flexural strength (Fig. 12). This study found that silica beams fabricated with the fastest scan speed tested (250 mm/s) exhibited higher strengths than those fabricated at slower speeds. This test also served to validate the above finding that an annealing temperature of 1250 °C results in parts with the highest flexural strength.

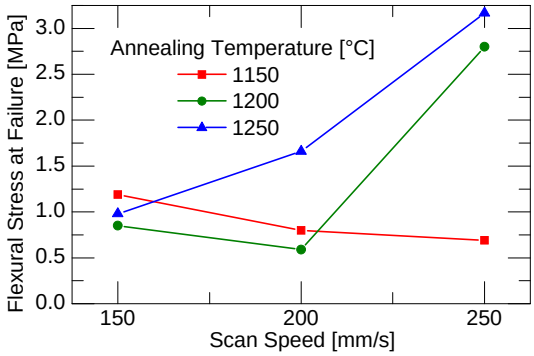

Fig. 12. Flexural strength of silica deposited at varying scan speeds

Conclusion

The SLS platform developed was used to manufacture complex three-dimensional geometries, some of which may also involve the fusion of previously un-connected structures (see Fig. 13). The parameters identified as producing optimal sintered structures are a laser power of 19.5 W and a scan speed of 200 mm/s. The density of the sintered silica associated with these parameters was found to be 0.4146 g/cm^3, following a mass loss of 0.0146±0.0032g during the sintering process. The density was further increased to 0.67 g/cm^3 by annealing the sintered silica at a temperature of 1250 °C for a soak time of thirty minutes. In addition to densifying the silica, the annealing process also resulted in increased flexural strength. In particular, a maximum flexural strength of 3.165 MPa was observed for parts annealed at 1250°C.

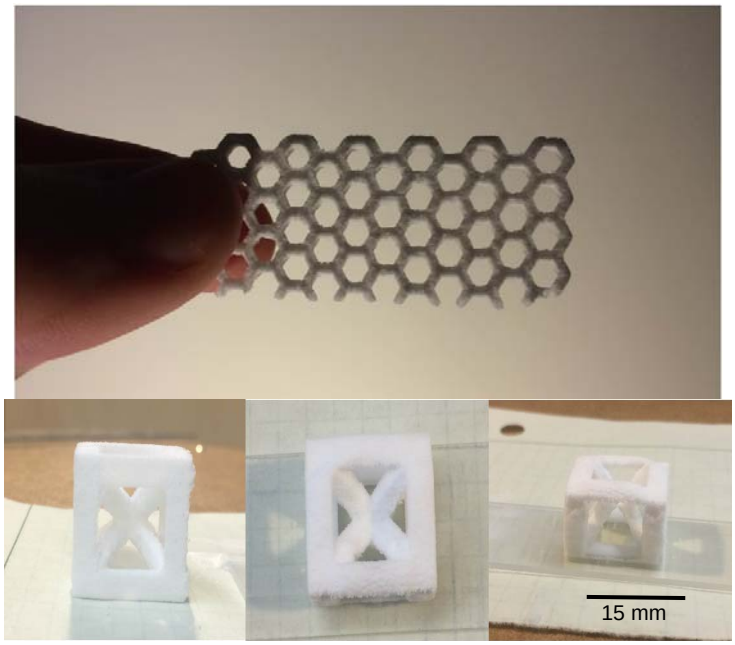

Fig. 13. Structures created via SLS platform (as-printed)

The sifter powder distribution method needs to be refined before further investigations into the fabrication of silica with SLS may be conducted. The large powder layer depth and variations in layer thickness limit the part's geometrical precision. This also results in variations in the mechanical strength of silica parts which is likely to impact the observed trends. Work should be done to improve powder distribution by attaching the sifter to the carriage on the gantry in the SLS platform to allow a consistent amount of powder to be deposited for each layer, as well as to increase the control over the depth of the deposited powder layer.

The high porosity of the parts complicated the traditional Archimedean method for determining a part's volume[13]; which necessitated a volume approximation via electronic calipers instead. A more accurate means for determining the volume of deposited silica parts would result in more accurate calculations of flexural strength. Also, it should be investigated whether or not further densification occurs for annealing temperatures greater than 1250°C and for soak times greater than thirty minutes, as further densification may also correlate to an increase in flexural strength.

Acknowledgements

The author would like to thank Dr. Jeremy Watts, from the Missouri University of Science and Technology Materials Research Center for help with the flexural testing as well as Chuang Qu and Brett Buswell, also from Missouri S&T for useful discussions.

References

[1] M. Fateri, A. Gebhardt, S. Thuemmler, L. Thurn, "Experimental investigation on Selective Laser Melting of Glass." *Physics Procedia*, **56**, 357-364 (2014).

[2] S. Kumar, "Selective Laser Sintering: A Qualitative and Objective Approach", *JOM Journal of Minerals, Metals and Materials*, **55**(10) 43-47 (2003).

[3] J.P. Kruth, X. Wang, T. Laoui, L. Froyen, "Lasers and materials in selective laser sintering", *Assembly Automation*, **23**(4) 357-371 (2003).

[4] R.S. Khmyrov, S.N. Grigoriev, A.A. Okunkova, and A.V. Gusarov, "On the Possibility of Selective Laser Melting of Quartz Glass" *Physics Procedia*, **56** 345-356 (2014).

[5] M. Fateri, A. Gebhardt, "Selective Laser Melting of Soda-Lime Glass Powder" *Int. J. Appl. Ceram. Technol.*, **12**(1) 53-61 (2015).

[6] J.P. Kruth, P. Mercelis, J. Van Vaerenbergh, "Binding mechanisms in selective laser sintering and selective laser melting", *Rapid Prototyping Journal*, **11**(1) 26-36 (2005).

[7] F. Klocke, H. Wirtz, "Selective Laser Sintering of Zirconium Silicate", Proc. Solid Freeform Fabrication Symposium, Austin, 605-612 (1998).

[8] Ph. Bertrand, F. Bayle, C. Combe, P. Goeuriot, I. Smurov, "Ceramic components manufacturing by selective laser sintering", *Applied Surface Science*, **254**(4) 989-992 (2007)

[9] F. Klocke, C. Ader, "Direct Laser Sintering of Ceramics", Proc. Solid Freeform Fabrication Symposium, Austin, 447-455 (2003).

[10] J.L. Song, Y.T. Li, Q.L. Deng, D.J. Hu. “Rapid prototyping manufacturing of silica sand patterns based on selective laser sintering”, *Journal of Materials Processing Technology* **187**, 614-618 (2007)
[11] Y. Tang, J.Y.H. Fuh, H.T. Loh, Y.S. Wong, L. Lu, "Direct Laser Sintering of a Silica Sand" *Materials and Design* **24**(8) 623-629 (2003).
[12] ASTM, “Standard Test Method for Flexural Strength of Advanced Ceramics at Ambient Temperature”, C1161 (2013)
[13] ASTM, “Standard Test Method for Density of Powder Metallurgy (PM) Materials Containing Less Than Two Percent Porosity”, B311–13 (2013)